ELSEVIER

Ecological Modelling 154 (2002) 263–288

ECOLOGICAL MODELLING

www.elsevier.com/locate/ecolmodel

Forest canopy hydraulic properties and catchment water balance: observations and modeling

V.C. Engel [a,*], M. Stieglitz [a], M. Williams [b], K.L. Griffin [a]

[a] *Lamont–Doherty Earth Observatory, 206 Oceanography, Route 9W, Palisades, NY 10964, USA*
[b] *Institute of Ecology and Resource Management, 115 Darwin, University of Edinburgh, Edinburgh, UK*

Received 27 August 2001; received in revised form 15 January 2002; accepted 4 March 2002

Abstract

We present observations and simulations examining plant–water relations in a forested catchment characterized by strong topographic control over surface hydrology and stand structure. The system is dominated by xeric and mesic ecotypes of *Quercus rubra* L. Soil depths are typically very thin and the severity of seasonal water stress in these trees is determined largely by position along the local topographic gradient. Water balance related ecotypic differences in *Q. rubra* were measured during the 2000 growing season at an upland and lowland site. Significant site differences in stomatal conductance, sap flux density, and leaf to sapwood area ratios were observed. However, mid-day leaf water potentials and the leaf area-specific canopy hydraulic conductance were not significantly different despite a 20% increase in soil moisture content, an average 10 m increase in tree height, and a higher leaf area index at the lowland site. These results suggest a close coordination of tree morphology, stand structure, and the hydraulic conductance of the combined soil–root–leaf pathway that governs leaf-level water vapor exchange rates similarly across the topographic gradient. To place these stand-level observations in the context of catchment-scale water balance we linked the SPA canopy model with a 1-D soil column model and TOPMODEL hydrologic formulations. The SPA model was used to represent the canopy because of its specific inclusion of hydraulic constraints on transpiration and leaf water potential. The combined model is spatially explicit in the distribution of ecotype morphology, and calculates transpiration rates for TOPMODEL-derived saturated and unsaturated area fractions within the watershed separately. Model predictions of stomatal conductance, upland latent energy flux, stream discharge, and soil moisture content compared favorably with observations. Sensitivity analyses of canopy model parameters indicate stream discharge in this system is most sensitive to changes in the maximum leaf area index, the minimum leaf water potential, and belowground resistance. Discharge was least sensitive to changes in stem hydraulic conductivity and capacitance. Model results and observations are discussed with respect to adaptations to water stress, hydraulic controls on canopy water use, and ecosystem water use. © 2002 Elsevier Science B.V. All rights reserved.

Keywords: Hydraulic conductance; Evapotranspiration; *Quercus rubra*; Water balance

* Corresponding author. Tel.: +1-845-365-8547; fax: +1-845-365-8156.
E-mail address: vengel@ldeo.columbia.edu (V.C. Engel).

0304-3800/02/$ - see front matter © 2002 Elsevier Science B.V. All rights reserved.
PII: S0304-3800(02)00068-6

1. Introduction

Stomata mediate a significant fraction of the annual flux of water between the soil and the atmosphere in forested catchments. Stomatal responses to environmental variables may best be understood in the context of the hydraulic conductance (G_t) of the soil–root–leaf system (Tyree and Sperry, 1988; Reich and Hinckley, 1989; Saliendra et al., 1995; Sperry et al., 1998; Oren et al., 1999). In forested systems, the control over G_t is the result of complex physiological and environmental mechanisms operating across several spatial and temporal scales. Short-term water stress generally results in stomatal closure and a reduction in canopy hydraulic conductance. Over the long term, plants adapt to site water balance through differential allocation to roots, stems, and leaves. These adaptations are necessary to maintain favorable leaf water potential (Ψ_L) during drought stress (Whitehead, 1998). Because these adaptations are intimately linked with photosynthesis and competition for resources, they also affect survival in mixed stands. The overall stand structure, therefore, reflects both the competition for resources and the dominant stresses imposed by the environment. Height (Schafer et al., 2000), rooting characteristics (Rieger and Litvin, 1999) and stand density (Whitehead et al., 1984) are a few of the canopy structural properties known to affect G_t and forest water use.

The hydraulic conductance of the soil–root–leaf pathway influences many land surface–atmosphere interactions and this has been the subject of numerous investigations (see Wullschleger et al., 1998 for review). Considering G_t more explicitly in hydrologic mass balance studies may also be instructive in further describing large-scale carbon and water fluxes and is the primary goal of this investigation. To achieve this it is necessary to consider both the hydraulic constraints on atmospheric fluxes and the topographic factors that govern soil moisture distribution and runoff in a consistent framework.

Many models have coupled canopy flux routines to soil water balance schemes (e.g. H2OTRANS (Knight et al., 1985); FOREST-BGC (Running and Coughlan, 1988); BEST (Pitman et al., 1991); CENTURY (Parton, 1993); SiB2 (Sellers et al., 1996); Whitehead et al., 2001). Several process-based hydrologic models do account for topographic controls over soil moisture conditions (e.g. TOPMODEL (Beven and Kirby, 1979); VIC (Liang et al., 1994); Band et al., 1993; Wigmosta et al., 1994; Stieglitz et al., 1997). In either case, these hydrologic models typically employ empirical (e.g. Jarvis 1976), rather than mechanistic formulations to predict stomatal conductance and canopy fluxes. Although these empirical functions have proven useful over a wide range of conditions, they clearly do not represent the dependence of stomatal conductance (and hence transpiration) on the hydraulic transport properties of the soil–root–leaf pathway. Therefore, linking process based hydrologic models with more mechanistic canopy models that simulate the dynamics of the soil–root–leaf pathway may provide improved predictions of large-scale water and carbon fluxes. To date, only a few modeling studies have used the hydraulic properties of the soil–root–leaf pathway to provide a semi-mechanistic basis for predicting stomatal conductance and canopy fluxes e.g. (Williams et al., 1996; Sperry et al., 1998; Law et al., 2000).

The objective in this paper is to establish the relationships that exist between stomatal conductance (g_s), Ψ_L, G_t, soil moisture distribution and site water balance in an experimental catchment dominated by mesic and xeric ecotypes of *Quercus rubra*. Our approach is two-fold. First, we start by analyzing water relations of this species at an upland and lowland site. The sites differ primarily with respect to soil moisture content (θ) and canopy structure. The adaptive significance of hydraulic architecture in these ecotypes is discussed and we examine similarities in the coordination of liquid and vapor phase conductance in upland and lowland communities. Then, we incorporate canopy structure and soil–root–leaf dynamics into the larger context of catchment water balance. To accomplish this we developed a simulation model that combines watershed dynamics (Stieglitz et al., 1997) with the SPA (soil–plant–atmosphere) canopy model (Williams et al., 1996, 2001). The hydrology model is based on TOPMODEL formulations and uses topographic data

and the average water table depth in the catchment to predict stream discharge (Q, m d^{-1}). At each time step the TOPMODEL formulations also predict the saturated fraction of the watershed (i.e. the area over which the water table is at the soil surface). Canopy fluxes are calculated independently for the saturated and unsaturated area fractions by running two SPA models in parallel, one representing the upland canopy and the other the lowland canopy. We used observational data on *Q. rubra* ecotypes from our upland and lowland field sites to parameterize the SPA canopy models. The SPA model was chosen to represent the canopy because at each model time step, Ψ_L is calculated for each canopy layer using G_t and includes detailed belowground subroutines necessary to represent the complete soil–root–leaf pathway. The model is validated using observations of g_s, canopy latent energy flux (LE, W m^{-2}), θ (cm^3 cm^{-3}) and Q. The sensitivity of Q to changes in the minimum leaf water potential (Ψ_{min}) and other SPA canopy hydraulic parameters is then tested. These sensitivity analyses provide a context for discussing the larger scale effects of soil–leaf–root dynamics and canopy hydraulic properties on catchment water balance.

2. Methods

2.1. Study site

The Black Rock forest is a 1500 ha preserve located in the Hudson Highlands region of New York (41°21′ N, 74°01′ E). Elevations in the forest range from 110 to 450 m above mean sea level (m.s.l.), with average seasonal temperatures from −2.7 °C in January to 23.4 °C in July. The medium texture soils are typically very thin, ranging from 10–15 cm in upland areas to greater than 1 m in the depressional areas. Soils in depressional areas are more organic than in upland areas, but bulk densities are not significantly different (K. Brown, unpublished data). Exposed bedrock is common throughout the preserve. Lumber extraction ceased in 1927 and the forest has been managed as a preserve without significant disturbance since that time. The system is typical of the *Quercus* dominated, secondary growth forests that have characterized the NE United States over the past century. There are approximately 734 trees per hectare throughout the forest with an average basal area of 21.0 m^2 ha^{-1} (Friday and Friday, 1985; W. Schuster, unpublished data). *Q. rubra* is the dominant species in the forest and represents 42.3% of the total basal area. *Quercus prinus* Willd. is the next most dominant species and represents 23.8% of the total basal area, followed by *Acer rubrum* (7.6%). The distribution and dominance of tree species along the elevational gradients within the forest roughly follows their drought tolerance. *Acer* spp., *Betula* spp., and *Fraxinus* spp. are present in lowland and depressional areas, while hill slopes and ridge tops are dominated primarily by *Quercus alba* and *Q. prinus*. Although it is dominant in the mesic areas, *Q. rubra* is significant in terms of basal area throughout the forest.

Research was focused in two 0.10 ha permanent research sites established across a topographic gradient in a 135 ha catchment within the Black Rock forest (Fig. 1). The upland site is approximately 140 m higher in elevation than the lowland site and is roughly 430 m above m.s.l. The distance between the two research plots is less than 1 km. Species dominance and composition in the two study sites are similar to forest-wide averages (Turnbull et al., 2001). At the lowland site, the average canopy height is 20–30 m, with dominant trees 30–50 cm in diameter at breast height (dbh). At the upland site, the canopy height is 10–16 m, with dominant trees averaging 20–30 cm dbh. The catchment is drained by a stream named Cascade Brook. Average hourly discharge rates from Cascade Brook are calculated using a pressure transducer installed behind a V-notch weir in 1998.

2.2. Site measurements

A 15 m tower was erected at the upland site in April, 1999 and equipped with meteorological instrumentation at a reference level (5 m) above the canopy. Air temperature (T_a, °C), vapor pressure (kPa, Dew-10 hygrometer, Campbell Scientific Instruments, Logan, UT, USA), wind speed and

direction (Model 034A, Met One Instruments, Inc. Grants Pass, OR, USA), and total solar radiation (LI-200SA, Li-Cor, Lincoln, NE, USA) were measured every 10 s and 20 min averages recorded on a CR10X datalogger supplemented by an AM25T and AM416 multiplexer (Campbell Scientific Instruments, Logan, UT, USA). Air temperature was measured using Type E thermocouples at two locations above the canopy. Hourly meteorological data were compiled and used to drive the model simulations described below. Average θ and soil surface temperatures (T_s, °C) were calculated from measurements at four locations at both sites. Four CS615 probes (Campbell Scientific Instruments, Logan, UT, USA) were used to measure θ. All CS615 probes were inserted into the upper 15 cm of soil matrix. Soil thermocouples were inserted into the top 10 cm of soil beneath the litter layer. The site differences in θ are largely determined by their location on the local topographic gradient.

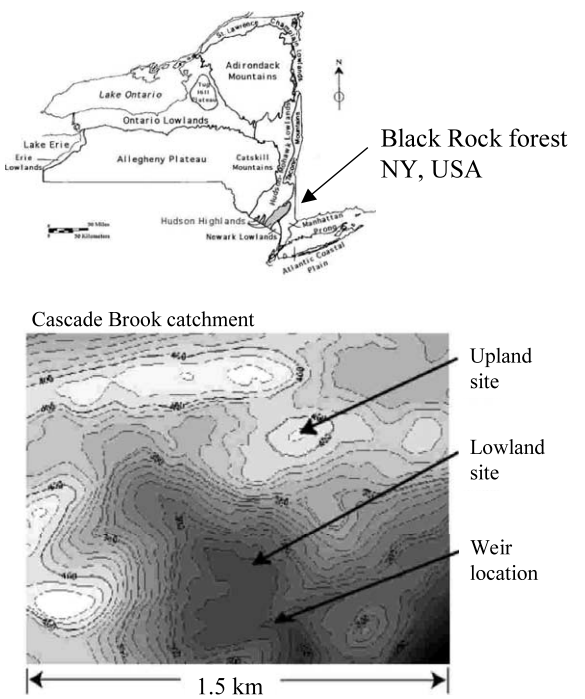

Fig. 1. Location of the Black Rock forest, near Cornwall, NY, USA and a topographic map of the catchment drained by Cascade Brook showing the location of the V-notch weir and the upland and lowland research sites.

Measurements of stomatal conductance (g_s, mol m^{-2} s^{-1}), sap flux density, and Ψ_L at the upland site were performed periodically throughout the 2000 growing season. An effort to concurrently measure these variables in dominant trees at both sites was undertaken between September 17th and 21st, 2000. Two portable systems (Li-Cor 6400, Lincoln, NE, USA) were used to measure g_s on a subset of *Q. rubra* trees at both sites. Measurements of g_s on upper canopy, primarily sunlit leaves were performed on September 20th and 21st, 2000 on a set of four trees at each site. A 10 m scaffolding and the 15 m meteorological tower were used to access the trees at the upland site. A 25 m hydraulic lift was used to access leaves from four *Q. rubra* trees at the lowland site during the September 2000 sampling effort. Measurements of g_s were taken on four fully expanded leaves from each tree as frequently as possible between 08:00 and 18:00 h. The clear cuvette attachment on the Li-Cor 6400 was used to ensure measurements were as close to in situ rates as possible. Measurements were recorded after gas exchange rates in the sample cuvette had stabilized (total coefficient of variation of ΔCO_2, ΔH_2O and flow rate over a 45 s period less than 1.0%) with respect to the reference cuvette.

Predawn and mid-day Ψ_L and g_s were measured concurrently on most sampling days. Four leaves from each tree were sampled ($n = 16$) at each study site, using a Scholander pressure bomb (PMS Instruments Inc., Corvalis, OR, USA). Soil water potential (Ψ_S, MPa) was estimated from predawn Ψ_L values adjusted for gravitational effects due to sampling height. Leaves at the same height as those used for g_s measurements were collected, sealed in aluminum foil packets, and measured within 20 min of removal. Mid-day Ψ_L values were recorded immediately following g_s measurements between 13:00 and 15:00 h EST.

Granier-type heat dissipation probes (Granier, 1985, 1987; Phillips et al., 1996) were used to measure sap flux density (U, kg m^{-2} sapwood area s^{-1}) in six *Q. rubra* trees at each site. The 20 mm probes and electrical circuitry were installed in sample trees in July 2000. Type T thermocouples inserted into each probe were monitored using an AM25T multiplexer and datalogger. One

Table 1
Sample tree dimensions in the Cascade Brook watershed

Tree #	Total basal area (cm^2)	Sapwood area (cm^2)
Upland trees[a]		
1	1017.4	107.3
2	1017.4	193.2
3	356.2	60.7
4	366.3	104.3
5	637.6	135.1
6	486.7	98.67
Lowland trees[b]		
1	1148.5	139.6
2	1519.7	152.5
3	1163.6	117.8
4	986.5	118.6
5	1411.2	127.9
6	510.5	46.5

[a] Measurement height 10 m.
[b] Measurement height 20 m.

heated and one reference probe were inserted into each sample tree approximately 15 cm apart. Fine-gauge constantan wire coiled around the heated probe dissipated a constant 0.2 W. Sap flux density was calculated (Granier et al., 1990) using the equation:

$$U = 0.116*((\mathrm{d}T_\mathrm{m} - \mathrm{d}T)/\mathrm{d}T)^{1.2} \quad (1)$$

where, $\mathrm{d}T_\mathrm{m}$ is the maximum temperature difference (°C) between the heated and reference probes during conditions of no flow (pre-dawn) and $\mathrm{d}T$ is the temperature differential during period of positive sap flow. Temperature differentials between the probes were 12–15 °C and 8–10 °C during periods of zero and positive sap flow, respectively. The $\mathrm{d}T$ values were corrected after Clearwater et al. (1999) to account for differences in the amount of sapwood in contact with the heated probes. Following the measurement period, tree cores were taken adjacent to the heated probes and the depth of sapwood measured visually to the nearest 0.5 mm. One set of probes was used for each tree. Table 1 lists the dimensions of the trees used to measure U at both sites.

Average values of U and Ψ_L were used to calculate two stand-level measures of canopy hydraulic properties at both sites. Stand-level hydraulic conductance (G_t, kg m^{-2} s^{-1} MPa^{-1}) of the combined soil–root–leaf pathway was calculated such that

$$G_\mathrm{t} = E/(\Psi_\mathrm{S} - \Psi_\mathrm{L} - h\rho g) \quad (2)$$

where E (kg m^{-2} s^{-1}) is the total stand transpiration per unit ground area, and $h\rho g$ is the correction term based on tree height, h (m), the density of water ρ (g m^{-3}) and gravitational acceleration (g). The stand relative conductivity (k, m^2) was calculated such that,

$$k = \frac{10^{-3} E h \eta}{(\Psi_\mathrm{S} - \Psi_\mathrm{L} - h\rho g)} \quad (3)$$

where η (MPa s^{-1}) is the viscosity of water at 20 °C, and the factor 10^{-3} converts the value of E to m s^{-1}. For stand-level calculations, E was determined at each site using the average U for all sample trees multiplied by the site sapwood area index (SAI, m^2 sapwood area per m^2 ground area). To determine the SAI, the sapwood area (A_S) was first estimated for each sample tree from the average of four cores removed at the same height where sap flux was measured. The slope of a simple linear regression between the basal area (A_T) and A_S for all sample trees was used to determine the sapwood to basal area ratio (A_S:A_T) at each site ($r^2_\mathrm{uplands} = 0.87$; $r^2_\mathrm{lowlands} = 0.83$). These A_S:A_T values were then multiplied by the stand-level basal area (m^2 stem area per m^2 of ground area) for each site to determine the upland and lowland SAI. At each site, the leaf area to sapwood area ratio (A_L:A_S) was determined by dividing the leaf area index (LAI m^2 leaf area m^{-2} ground area; determined from litter trap data) by SAI.

Stand-level hydraulic conductance was normalized by leaf area ($G_\mathrm{t,LA}$, kg m^{-2} s^{-1} MPa^{-1}) using the equation:

$$G_\mathrm{t,LA} = E/(\Psi_\mathrm{S} - \Psi_\mathrm{L} - h\rho\,\mathrm{g})*1/\mathrm{LAI} \quad (4)$$

The slopes of linear regressions based on Eqs. (2)–(4) were used to calculate G_t, k, and $G_\mathrm{t,LA}$ for each site. Values for E, $Eh\eta$, and E/LAI were plotted against stand average soil–leaf water potential gradients ($\Psi_\mathrm{S} - \Psi_\mathrm{L} - h\rho g$) for 7 sample days and the slopes of regressions through these plots were used to determine G_t, k, and $G_\mathrm{t,LA}$, respectively. Intercepts were forced through the

origin for all regressions and calculations were performed separately for each site. Calculations of G_t, k, and $G_{t,LA}$ were performed using only mid-day Ψ_L and steady-state sapflow data.

A Bowen ratio energy balance system (Campbell Scientific Instruments, Logan, UT, USA) was used to estimate LE at the upland site during the 2000 growing season. The Bowen ratio method estimates LE using the following set of equations:

$$LE = (R_n + G)/(1 + \beta) \quad (5)$$

where, R_n is the net radiation (W m^{-2}) at the reference height above the canopy, G is the ground heat flux (W m^{-2}), and β is the Bowen ratio of sensible heat flux (S, W m^{-2}) to LE, such that:

$$\beta = \frac{\gamma(dT_a)}{dVP} \quad (6)$$

where dT_a is the vertical air temperature gradient (K) above the canopy, dVP (kPa) is the vertical vapor pressure gradient over the same distance, and γ is the psychometric constant (kPa K^{-1}). Two Type E fast-response thermocouples were used to measure dT_a, and dVP was measured using the Dew-10 hygrometer. The upper and lower sample points used to measure dT_a and dVP were 4.5 m apart with the lower point 0.5 m above the canopy. The hygrometer automatically switches intakes between the upper and lower sample points to avoid systematic sensor errors. The thermocouple configuration for this system did not deviate significantly from the manufacturer's specifications. Net radiation was measured using a Q*7.1 (REBS, Seattle, WA) positioned at the height of the upper sample point. Soil heat flux, G, was taken as the average of two HFT-3.1 plates (REBS, Seattle, WA, USA) placed approximately 8 cm below the litter layer. Observations of all parameters necessary to compute LE were measured at a frequency of 0.1 Hz and the data averaged to give hourly values. Only daytime LE values were considered.

In order to use the Bowen ratio method to estimate LE, adequate upwind fetch relative to the difference between the measurement height and the zero-plane displacement ($0.75h$) is necessary. While the canopy itself is continuous and species composition does not change appreciably with respect to commonly accepted fetch:height requirements (e.g. 100:1), the Black Rock Forest is characterized by moderate topographic relief. Care was taken to place the Bowen ratio tower in the most topographically homogenous area in the watershed, near the top of the elevational gradient. Oke (1987) provides a thorough description of the effects of topographic features on land surface–atmosphere interactions and considers slopes of less than 17% insufficient to cause boundary layer separation during moderate wind speeds. We estimated our fetch:height ratios using a criterion of 10% change in elevation in upwind directions. Wind direction during the 2000 growing season was predominately from the WNW. Changes in elevation greater than 10% do not occur within 0.3 km in this direction. Using a 7.5 m difference between the zero-plane displacement and the reference measurement height, this provides a fetch:height value of 40:1 in this direction. (See Herbst (1995), Irvine et al. (1997), Heilman et al. (1989) for comparable fetch:height values applied in Bowen ratio analyses).

3. Model description

3.1. TOPMODEL formulations

Many hydrology models have been developed using TOPMODEL formulations (Beven and Kirby, 1979; Sivapalan et al., 1987; Ambroise et al., 1996; Stieglitz et al., 1997). A framework of analytic equations, TOPMODEL is based on the idea that topography is the primary determinant of the distribution of soil moisture at and within the land surface (Beven and Kirby, 1979; Beven, 1986).

TOPMODEL formulations define areas of hydrological similarity—that is, points within a watershed that respond to meteorological forcing in similar fashion, saturating to the same extent, producing the same levels of discharge, etc. These points of hydrological similarity are identified by an index that is derived from analysis of catchment topography. This topographic index is often of the form $\ln(a/\tan\beta)$, where $\tan\beta$ is the local

slope angle at a point on the land surface, and 'a' is the amount of upslope area draining through that point. Consequently, lowland areas tend toward higher topographic index values, due to a combination of either low slope angle or large upslope area. Upland areas tend conversely toward lower topographic index values. Points within a catchment defined by the same topographic index value are assumed to respond identically to atmospheric forcing. Thus within a TOPMODEL framework, the topographic index provides the fundamental unit of hydrological response.

This fundamental topographic unit is derived from three basic assumptions (see Ambroise et al., 1996; Beven, 1997 for details): (1) the water table is nearly parallel to the soil surface so that the local hydraulic gradient is close to $\tan\beta$; (2) the saturated hydraulic conductivity falls off exponentially with depth; and (3) the water table is recharged at a spatially uniform, steady rate that is slow enough, relative to the response time scale of the watershed, to allow the assumption of a water table distribution that is always at equilibrium. These assumptions permit reconstruction of the spatial variability of catchment response to meteorological forcing solely from modeling of the response of the mean state. This quasi-stochastic approach is at once computationally efficient while still permitting dynamic representations of physical processes within the system.

3.2. The hydrology model

The hydrology model employed for this study has been previously described (Stieglitz et al., 1997). Briefly, two methods are used for modeling the flow of water within a catchment. The first is a soil column model that simulates the vertical movement of water and heat within the soil and between the soil surface plus vegetation to the atmosphere. The ground scheme consists of ten soil layers. Layer thicknesses are in a geometric series determined from the depth of the first ground layer. Diffusion and a modified tipping bucket model govern heat and water flow, respectively. The prognostic variables, heat and water content, are updated at each time step. In turn, the fraction of ice and temperature of a layer may be determined from these variables.

The second method partitions the catchment surface into two distinct hydrologic zones: saturated lowlands; and unsaturated uplands. Using the statistics of the topography, the horizontal movement of groundwater is tracked from the uplands to the lowlands (a TOPMODEL approach). Combining these two approaches produces a three-dimensional picture of soil moisture distribution within a catchment. The partitioning of runoff and surface water and energy fluxes is effected without the need to explicitly model the landscape. Specifically, an analytic relation, derived from TOPMODEL assumptions, exists between the mean water table depth ($\bar{z}$) determined from the soil column model, and local water table depth at any location x (z_x) (Sivapalan et al., 1987 Wood et al., 1990)

$$z_x = \bar{z} - 1/f[\ln(a/\tan\beta)_x - \lambda] \tag{7}$$

where $\ln(a/\tan b)_x$ is the local topographic index at location x; λ is the mean watershed value of $\ln(a/\tan b)$, f (m^{-1}) is the rate of decline of the saturated hydraulic conductivity with depth in the soil column, and z is positive with depth.

By setting z_x equal to zero, i.e. locating the local water table depth at the surface, saturated regions of the land surface can be identified. This partial contributing area includes all locations for which

$$\ln(a/\tan\beta)_x > \lambda + f\bar{z} \tag{8}$$

From this partitioning, the contributions to river runoff of both precipitation directly onto stream channels and overland flow (saturation–excess runoff) can be quantified.

Groundwater flow is accounted for by baseflow—that is, the gradual relaxation of the water table from the uplands to the lowlands. Following Sivapalan et al. (1987), baseflow (Q_b) is:

$$Q_b = \frac{AK_{sat}(z=0)}{f}\, e^{-\lambda} e^{-f\bar{z}} \tag{9}$$

where A is the area of the watershed and K_{sat} is the saturated soil hydraulic conductivity at the surface. The flow represented by Q_b through the

soil matrix supports river discharge between storm events.

This combined approach to modeling the land surface has been validated at several watersheds, ranging in scale from 2.2 km^2 (Stieglitz et al., 1997) to 570 000 km^2 (Ducharne et al., 2000). The hydrology model employed in this study also includes a three layer snow model.

Finally, following Shaman et al. (2001), we adopt two new modeling strategies. First, a methodology for representing the physical process of stormflow within a TOPMODEL framework has been developed. Regions of near saturation (unsaturated) develop during storm events are now allowed to contribute to soil column discharge. That is, we now permit for a baseflow contribution from unsaturated zones. Determination of the stormflow contribution to discharge is made using the TOPMODEL equation for groundwater flow. A second modification is a reduction of porosity and field capacity with depth in the soil column. Large storm events are better captured and a more dynamic water table develops with application of this modified soil column profile. The modified soil column profile predominantly reflects soil depth differences in upland and lowland regions of a watershed. Combined, these two model modifications—stormflow and the modified soil column profile—provide a more accurate representation of the time scales at which soil column discharge responds and a more complete depiction of hydrologic activity.

3.3. The SPA canopy model

The original SPA canopy model (Williams et al., 1996) and its updated belowground subroutines (Williams et al., 2001) have been previously described. The model has been applied in diverse systems and validated with canopy scale fluxes of LE and CO_2 (Williams et al., 1996, 2001). The SPA model uses an iterative formulation to simultaneously determine photosynthesis (P_n, μmol CO_2 m^{-2} leaf area s^{-1}) and Penman–Monteith transpiration (E_n, mmol H_2O m^{-2} leaf area s^{-1}) rates for sunlit and shaded leaves based on the canopy hydraulic transport capacity. The model also includes a radiative transfer scheme. The original SPA routines for calculating g_s, P_n, E_n, leaf boundary layer conductance (g_{bl}), Ψ_L, and leaf temperature (T_L) were kept intact for these simulations. The radiative transfer scheme, and the routines for calculating precipitation throughfall, interception and evaporation from wet leaves were also retained. For each canopy layer n, the change in Ψ_L over time is calculated in SPA based on the following equation:

$$\delta\Psi_{L,n}/\delta t = \frac{\Psi_{SW} - h\rho g - E_n(R_{b,n} + R_{p,n}) - \Psi_{L,n}}{C_n(R_{b,n} + R_{p,n})} \quad (10)$$

where C_n is the layer capacitance, $R_{b,n}$ (MPa s m^2 $mmol^{-1}$) is the total belowground hydraulic resistance and $R_{p,n}$ (MPa s m^2 $mmol^{-1}$) is the total plant stem resistance for each layer. Penman–Monteith transpiration, E_n, is calculated for each canopy layer using g_s, net radiation at the leaf surface, atmospheric VPD and g_{bl}. The canopy model uses an iterative routine to solve for g_s such that the mesophyll CO_2 concentration matches the value predicted by two processes: (1) diffusion from the atmosphere and (2) metabolic uptake based on the Farquhar model parameters of the maximum rate of carboxylation (V_{cmax}, μmol CO_2 m^{-2} s^{-1}) and the maximum rate of electron transport (J_{max}, μmol CO_2 m^{-2} s^{-1}). Net radiation at the leaf surface is supplied by the radiative transfer scheme. Leaf boundary layer conductance, g_{bl}, is a function of windspeed and leaf dimensions (Jones, 1992). Stomatal conductance is calculated such that E_n is maintained at a rate that prevents Ψ_L from falling below the minimum allowable level (Ψ_{min}). For each time step, g_s is increased incrementally until either $\Psi_L = \Psi_{min}$ or the percentage increase in P_n is less than a hypothetical value termed the stomatal threshold parameter (l, 0.01%). This parameter controls the sensitivity of stomata to increases in P_n and hence controls water use efficiency. Once $\Psi_L = \Psi_{min}$, E_n is calculated such that $\delta\Psi_L/\delta t = 0$. The final value of Ψ_L for each layer is retained for the following time step. The total canopy latent energy flux is the sum of E_n in all layers plus direct evaporation of intercepted precipitation. The model was run for this application with ten canopy layers on an hourly time step.

3.4. The coupled model

A schematic diagram of the coupled model used for these simulations is illustrated in Fig. 2. The representation of SPA in this diagram is simplified. The iterative routine at the top of the diagram used to calculate P_n, Ψ_L, g_s, and E_n is replicated for the sunlit and shaded fractions of each of the ten canopy layers. See Williams et al. (1996) for a more detailed graphical representation of the canopy scheme. Belowground SPA routines are also simplified in Fig. 2; however, the root distribution sub-routines and the determination of root resistances were kept intact from Williams et al. (2001). Soil properties and physical processes are represented with the ten-layer soil column model of Stieglitz et al. (1997).

The model is parameterized with independent upland and lowland canopy morphologies, root distributions and leaf chemistry (Table 4). The parameters used to initialize the SPA canopy model were either measured directly in the field, taken from the literature, or estimated based on values used in previous SPA simulations at Harvard Forest (Williams et al., 1996). Species composition in the Cascade Brook watershed is similar to that found at Harvard Forest such that many of the same canopy model parameters could be applied to both systems. Fluxes in the TOPMODEL-derived unsaturated fraction (f_{unsat}) employ the morphology of the upland canopy, while fluxes in the saturated fraction (f_{sat}) employ the morphology of the lowland canopy. Because the soil model is 1-D, the upland and lowland canopies are both coupled through their root distributions to the same soil column. However, stomatal conductance, transpiration and Ψ_L are calculated separately for the two canopy models. To accomplish this, the weighted soil water potential (Ψ_{SW} in Williams et al., 2001) and the total belowground hydraulic resistance values (R_b—linear sum of root (R_r) and soil (R_s) resistances) required by SPA to determine Ψ_L (Eq. (10)) are calculated separately for f_{sat} and f_{unsat}. In saturated areas, R_b is an inverse function of root biomass and root resistivity (R_r^*, MPa s g mmol^{-1}) while R_s is set to zero. In unsaturated areas, R_b includes the R_s term as a function of soil hydraulic conductivity (k_{soil}, m s^{-1}, provided by the soil column model), total root length, fine-root radius, and the mean distance between roots (after Newman, 1969). Soil water potential in saturated areas is set to zero. In unsaturated areas, soil water potential is based on moisture content and the Brooks–Corey formulations as in Stieglitz et al. (1997). Transpiration fluxes from f_{sat} are removed directly from the soil layer that contains the water table, while transpiration withdrawals in f_{unsat} are partitioned (after Williams et al., 2001) amongst the soil layers that contain roots. The soil layer that contains the water table is determined using the TOPMODEL formulations.

The percentage of the total catchment area covered by upland and lowland canopy types is prescribed in the model initialization. Because the TOPMODEL-derived saturated fraction expands and contracts with the average water table depth, conditions arise when f_{sat} does not equal the fraction of the area covered by the lowland canopy type. During these periods, it is necessary to run three canopy models in parallel—all of which remove transpired water from the 1-D soil column. If f_{sat} is less than the area covered by lowland canopy type, a portion of the lowland canopy is subject to a soil column reflective of the mean state of the watershed. That is, belowground resistance (R_b) and soil water potential (Ψ_{SW}) for the lowland canopy outside f_{sat} are calculated as in the upland canopy. The root distributions and morphology of the lowland canopy subject to an unsaturated soil column are not changed, however, so that R_b and other canopy hydraulic characteristics (e.g. LAI, capacitance) are different from the upland type. A similar situation arises when f_{sat} is greater than the lowland canopy areal coverage. During these periods, a portion of the upland canopy is subject to a saturated soil column and the belowground processes are calculated as in the lowland, saturated zones. For the conditions during which the upland canopy is subject to a saturated soil column, the total belowground resistance is a function only of R_r, and Ψ_{SW} is set to zero. For model comparisons with observations below, simulation results from the upland-type canopy in

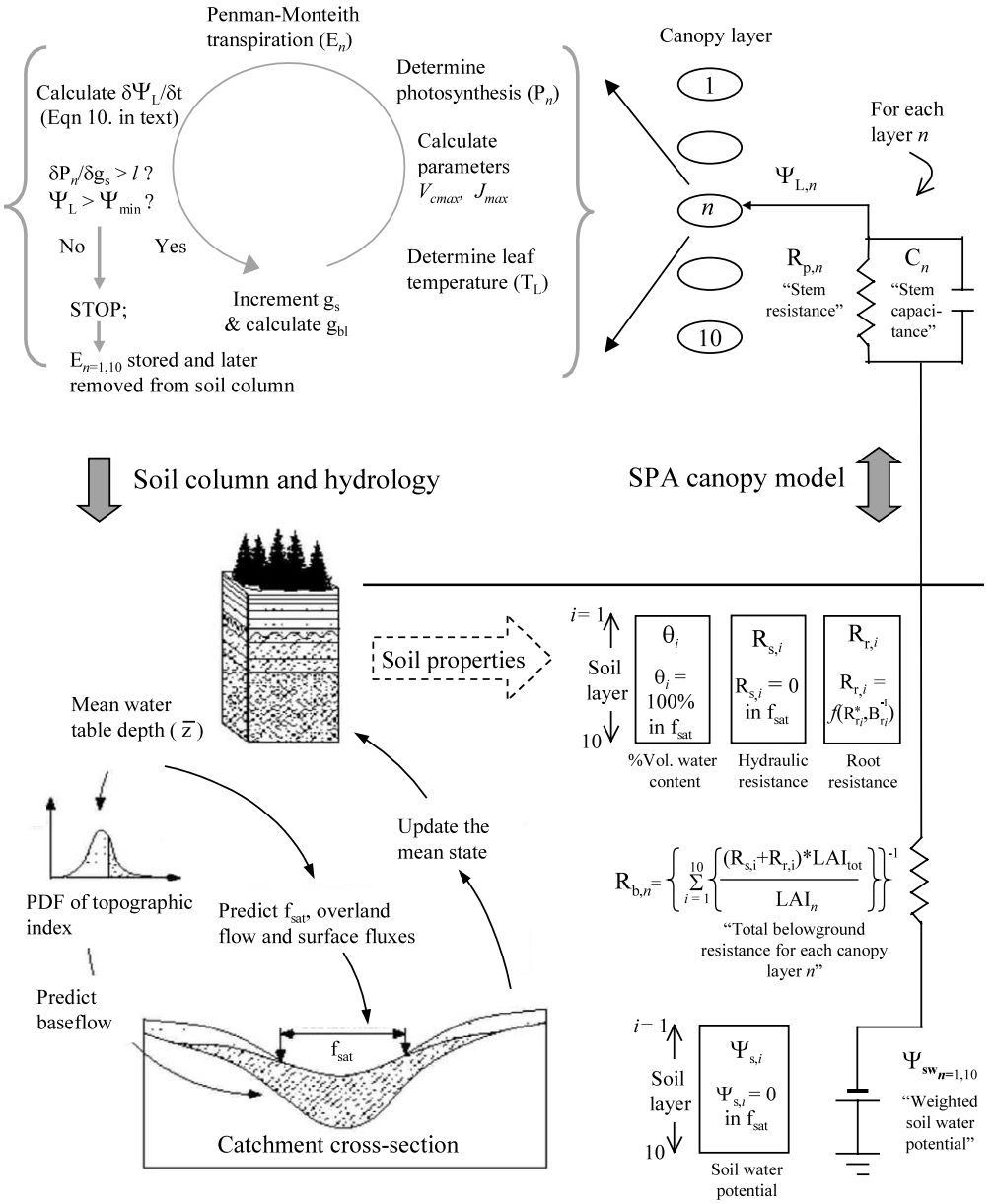

Fig. 2. Schematic diagram of the coupled SPA canopy, soil column and hydrology models used for simulations. The iterative routine at the top of the diagram is repeated for the sunlit and shaded fractions of each of the ten canopy layers. Leaf water potential (Ψ_L) is calculated in each layer according to Eq. (10) in the text. Within each time step, the model gradually increases stomatal conductance (g_s) until either the increase in P_n is less than a critical value (l) or Ψ_L equals Ψ_{min}. Total belowground resistance for each canopy layer ($R_{b,n}$) is the linear sum of soil (R_s) and root (R_r—a function of root resistivity, R_r^* and root biomass B_r) resistances for all soil layers weighted by the ratio of leaf area in the layer (LAI_n) to the total canopy leaf area (LAI_{tot}). Transpiration withdrawals from the soil column and the calculation of the weighted soil water potential (Ψ_{SW}) as in Williams et al. (2001). TOPMODEL formulations use the mean water table depth ($\bar{z}$) and a probability density function (PDF) of topographic data to predict the saturated fraction of the watershed (f_{sat}), overland flow, and baseflow. The updated water table depth is carried into the next time step for interaction with SPA model belowground subroutines. Two canopy models with distinct morphologies are included—one representing the lowland canopy with soil conditions as in f_{sat}; the other representing the upland canopy with soil conditions representing the mean state of the catchment.

unsaturated soil conditions will be compared to observations from the upland sampling site. Simulation results from the lowland-type canopy in saturated conditions will be compared to observations from the lowland sampling site.

A constraint on the system level energy balance was not included in this modeling exercise. As in the original SPA model, T_L for each canopy layer is determined using a steady-state approximation based on g_{bl} and the leaf surface energy balance (Jones, 1992). Leaf temperature however, is not included in the internal radiative transfer scheme. All leaves radiate to the layers above and below at the input ambient air temperature. The VPD of the air internal to the canopy—identical for all levels—is updated every hour using meteorological data and like air temperature, is unaffected by the leaf-level sensible and latent heat fluxes. While we did not quantify the error in system level energy balance associated with these simplifications, model predictions of soil surface temperatures agree well with observations (see Section 4). This was considered a qualitative confirmation that the error associated with this approximate energy balance scheme was relatively small. Care was taken, however, to ensure water balance in the model system. Heat and water fluxes within the ground scheme and between the ground surface and the internal canopy air follow Stieglitz et al. (1997).

The model was driven with meteorological data collected from the tower at the upland site from April 1999 to November 2000. Data provided by Black Rock Forest staff from a nearby station were used for the simulations covering the period from January 1998 to April 1999. All precipitation values were recorded using a tipping bucket (TE 525 Texas Electronics, Dallas, TX) located in a clearing approximately 4 km from the stream gauge. Hourly averages of total solar radiation (W m^{-2}), precipitation (m s^{-1}), windspeed (m s^{-1}), VPD (kPa), T_a (°C), and incoming longwave radiation (W m^{-2}), are read in at the beginning of each time step. The model requires approximately 1.5 min CPU time per year on a 600 MHz Pentium processor.

Incoming longwave radiation was calculated following Anderson and Baker (1965) using their aerosonde-based correction factor derived from surface and upper atmosphere humidity values measured over Vermont. The "cloudiness index" required in the Anderson and Baker (1965) model was calculated by dividing 2-week local maximums in daily-integrated total solar radiation by daily values measured at the upland site. The resulting longwave radiation averages about 100 W m^{-2} below theoretical blackbody values calculated from T_a and the Stefan–Boltzman formulation.

4. Results

4.1. Stomatal conductance

Fig. 3 shows g_s values recorded concurrently at the upland and lowland sites on September 20 and September 21, 2000 as a function of above-canopy VPD. During these two sampling days, values of g_s in upland trees were consistently lower than those recorded on lowland trees. The greatest differences in g_s between sites occurred at low VPD during early morning hours. The sensitivity of g_s to VPD was greater at the lowland site, and led to a convergence of values above 1 kPa at the two sites. In general the sensitivity of g_s to VPD in both the upland and lowland trees increased with soil drying following a rain event. The increase in VPD-sensitivity induced by soil drying was greater at the lowland site, however, and lead to significantly different g_s responses to VPD on September 21st—approximately 36–48 hours after the September 19th rain event.

4.2. Sap flux density

The average sap flux density, U, at the two sample sites for 7 days during the 2000 growing season are shown in Fig. 4. Trees at the upland site showed lower U rates than trees at the lowland site, but sustained rates close to maximum values longer through the day. The pattern in lowland trees is one of early maximum in U during the morning hours and a steady decline

throughout the day. The upland site is exposed to direct sunlight prior to the lowland site due to its location, and sapflow generally occurs earlier in the trees at this location. The sharp mid-day decline in U at both sites on September 19th was due to a rain event.

4.3. Leaf water potential

Average Ψ_S and mid-day Ψ_L values for upland and lowland trees are presented in Table 2. Values of Ψ_S at the upland site were slightly more negative ($\sim$0.1 MPa) than the lowland site reflecting differences in θ. A Student's t-test comparison was used to determine any significant site differences in mid-day Ψ_L on each sampling day. Significant differences ($P < 0.05$) in mid-day Ψ_L values occurred on September 3rd. All other days showed no significant differences. The Ψ_L and Ψ_S values presented in Table 2 were used to determine the soil–leaf water potential gradients in the calculations of G_t, k, and $G_{t,LA}$.

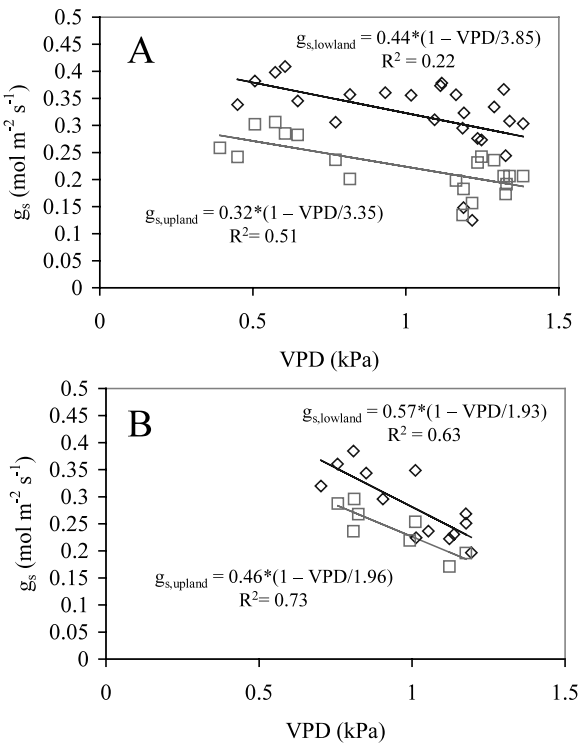

Fig. 3. Comparison of stomatal conductance rates in sunlit leaves in upland (squares) and lowland (diamond) trees on (A) September 20th and (B) September 21st. Data points are the averages of 16 measurements (four leaves per tree, four trees per site). A rain event on the evening of the 19th reduced water stress on the 20th relative to the 21st. Data were fit with using the expression $g_s = g_{s,max}(1 - VPD/VPD_0)$. Slopes of all fitted lines are significantly different from zero at ($P < 0.05$). Slopes of fitted lines in (B) are significantly different ($P < 0.05$) from each other.

4.4. Individual and stand-level hydraulic properties

Sap flow-based estimates of stand-level transpiration per unit leaf area and per unit ground area are plotted against the average soil–leaf water potential gradients in Fig. 5. The inverse slopes of the linear regressions fitted through these data were used to calculate G_t (Fig. 5A, Eq. (2)) and $G_{t,LA}$ (Fig. 5B, Eq. (4)) at each site. The same method was used to calculate stand hydraulic conductivity (k, plotted data not shown). The values for k, G_t, and $G_{t,LA}$ derived from these analyses are presented in Table 3. The lowland canopy showed significantly higher hydraulic conductance, G_t than the upland canopy reflecting the greater size of the individuals and the availability of water at this site. However, the site differences in stand hydraulic conductance per unit leaf area, $G_{t,LA}$, were not significant. Stand-level hydraulic conductivity, k, was significantly different between sites.

Table 3 presents several other stand- and individual-level properties of *Q. rubra* at the two sampling sites. The lowland site is characterized by fewer, but larger trees than those at the upland site (Friday and Friday, 1985; W. Schuster, unpublished data). The lowland site also supports trees with greater LAI and higher specific leaf areas. The trees at the upland site have diameters approximately one-half that of the lowland trees, but on average contain similar amounts of total sapwood area. As a result, the average sapwood to total basal area ratio (A_S:A_T) for individual trees at the upland site was double that of the lowland trees. Leaf–soil–leaf water potential gradients at the upland site were slightly higher, but not significantly different ($P < 0.05$) than at the lowland site. The maximum stomatal conductance

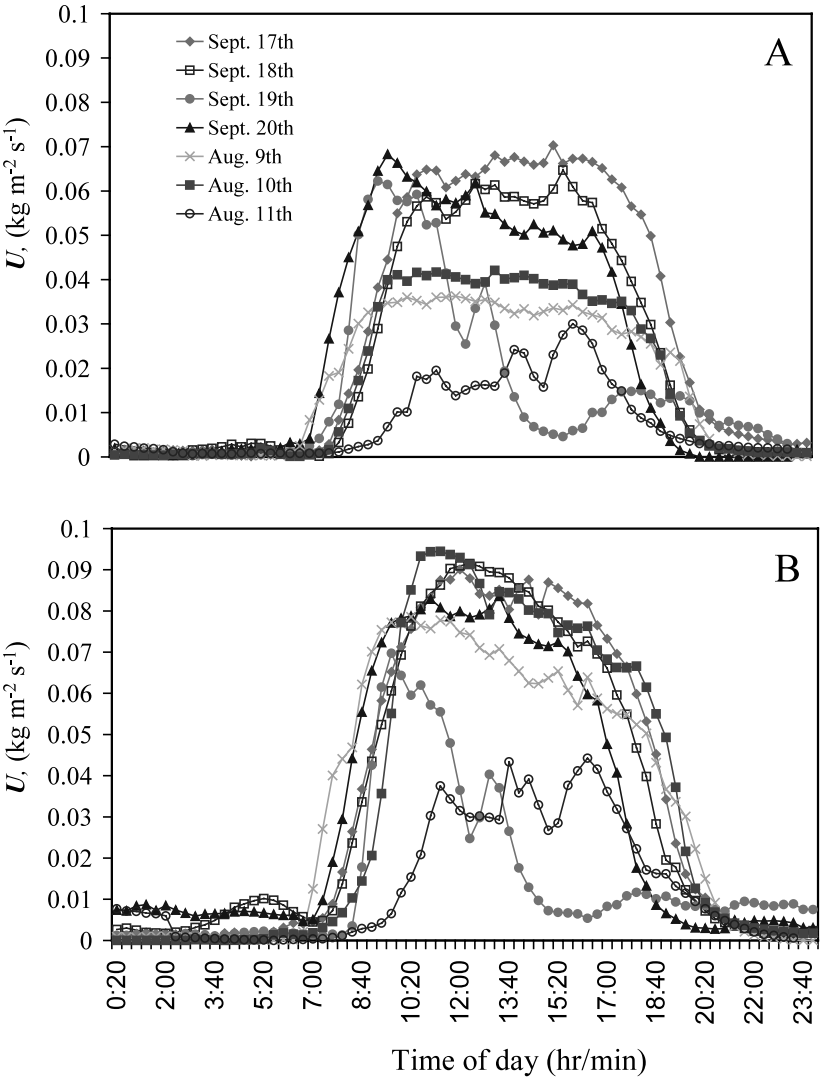

Fig. 4. Comparison of diurnal sap flux patterns in upland and lowland trees. Values represent average (six trees per site) sap flux density (U, kg m^{-2} s^{-1}) in trees at (A) the upland site and (B) the lowland site from 7 days during the 2000 growing season.

rate in *Q. rubra* recorded at the lowland site was higher than that recorded at the upland site.

4.5. Model results

The default parameter values for the SPA canopy models representing upland and lowland canopy types are listed in Table 4. Model results used for comparisons with observational data were generated using these values. A comparison of modeled and observed upper-canopy g_s values for upland and lowland canopies is presented in Fig. 6. In general, the modeled g_s values are similar to observations. The modeled response of g_s to diurnal changes in VPD is also similar to observations, with the exception of the lowland canopy simulations on September 21st. Stomatal conductance was less responsive to VPD on the 20th compared to the 21st. A rain event on the 19th, which lowered overall water stress, was re-

sponsible for the decreased sensitivity of g_s to VPD on the 20th.

Fig. 7 shows model estimates of upland, canopy level LE fluxes and observations for a 45-day period. Only daytime observations are presented. Nighttime LE fluxes were not calculated from observations and are graphed as zero values. Model results are most consistent with observations during periods of low LE flux. The timing and magnitude of the morning rise and evening decline of LE flux are captured well. Peak LE fluxes showed less agreement. The linear r^2 correlation coefficient of simulated-observed LE fluxes is 0.4. The majority of the discrepancies between model results and observations are during mid-afternoon and during periods of increased wind speeds.

Modeled, catchment-wide daily averaged values of soil temperature and moisture compare well with observations (Fig. 8). The model slightly overestimates soil temperature and slightly underestimates soil moisture. Fig. 9 shows the modeled and observed daily stream discharge rates. While modeled recession rates in general agree with observations, the model is less effective in capturing peak events. A more detailed discussion regarding hydrologic simulations in this watershed can be found in Shaman et al. (2001).

The ratio of upland and lowland transpiration rates (mm h^{-1}) versus upland root zone soil moisture (θ_r cm^3 cm^{-3}) is presented in Fig. 10A. The same ratio is plotted against atmospheric VPD in Fig. 10B. The lowland canopy transpiration values displayed in Fig. 10 were generated from the portion of the lowland canopy restricted to the saturated fraction of the watershed. Soil water potential and soil hydraulic resistance in this area are both set equal to zero. Upland canopy transpiration rates are approximately 80% of lowland rates under moderate moisture stress conditions. Deviations occur during very low soil moisture conditions, when upland rates are more reduced relative to lowland rates. During conditions of high VPD, upland transpiration rates exceed lowland values.

Fig. 11 shows a comparison of upland and lowland canopy hydraulic conductance per unit leaf area. Upland canopy values are reduced relative to the lowland canopy (points above the 1:1 line) during periods of very low θ_r in upland areas. In general, upland hydraulic conductance per unit leaf area was equal to or greater than lowland values.

4.6. Sensitivity analyses

For the 1998–2000 growing seasons we assessed the sensitivity of discharge to changes in canopy hydraulic parameters (Fig. 12). The changes in model parameters tested in the analyses were

Table 2
Average mid-day leaf (Ψ_L) and soil (Ψ_S) water potential values collected at the upland and lowland sapling stations during the month of September 2000

Date	Upland trees			Lowland trees		
	Ψ_L	Ψ_S	n	Ψ_L	Ψ_S	n
Sept. 1	−2.0 (0.3)[a]	−0.3	8	−2.4 (0.3)[a]	−0.1	8
Sept. 3	−3.0 (0.06)[a]		16	−2.1 (0.2)[b]		8
Sept. 8	−1.8 (0.3)[a]	−0.3	16	−1.9 (0.3)[a]	−0.3	8
Sept. 9	−1.7 (0.1)[a]		16	−1.9 (0.5)[a]		8
Sept. 17	−2.3 (0.1)[a]	−0.3	16	−2.1 (0.04)[a]	−0.2	16
Sept. 18	−1.9 (0.1)[a]		16	−1.8 (0.1)[a]		16
Sept. 20	−2.3 (0.2)[a]	−0.3	16	−2.2 (0.09)[a]	−0.2	16
Sept. 21	−1.9 (0.2)[a]		16	−1.8 (0.07)[a]		16

Similar letters indicate statistically similar ($P<0.05$) values of mid-day leaf water potentials across rows. Standard errors of measurement are enclosed in parentheses.

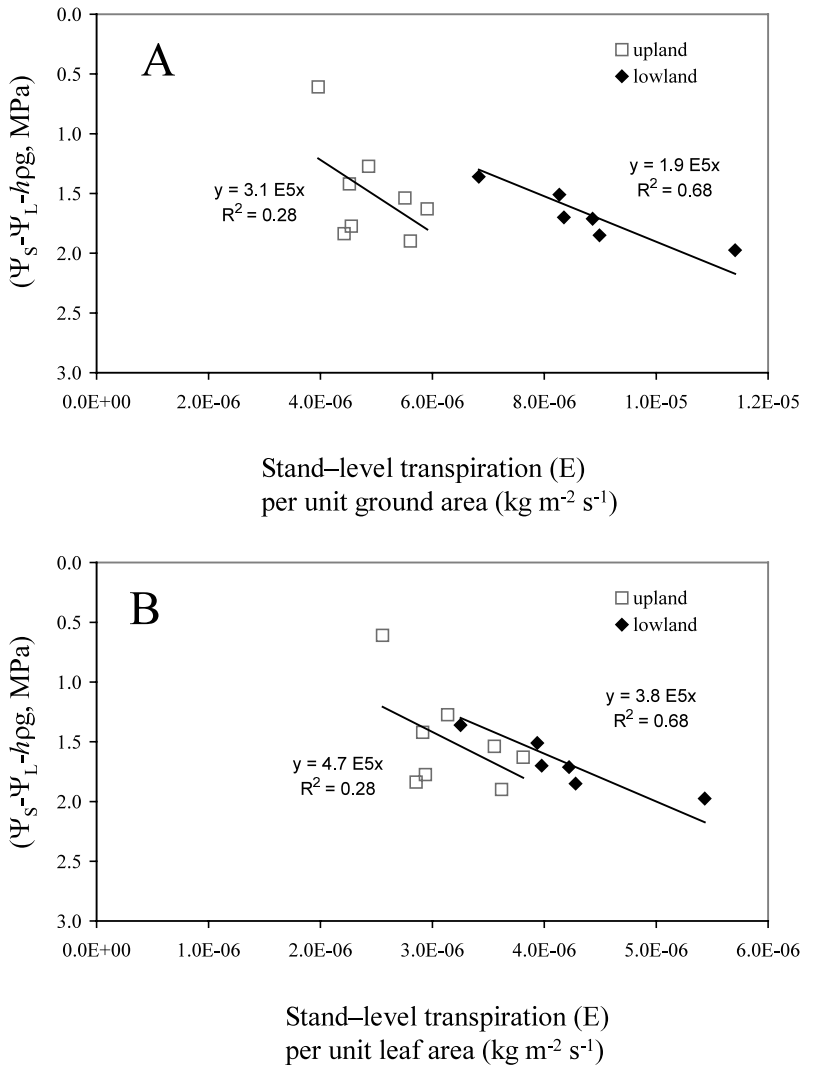

Fig. 5. Stand-average soil to leaf water potential gradients for upland (squares) and lowland (diamonds) canopies plotted against (A) transpiration per unit ground area and (B) transpiration per unit leaf area. Each data point represents a separate sampling day. Transpiration rates were derived from sap flux data taken from six trees at each site recorded during the period over which the mid-day leaf water potentials were measured. Mid-day leaf water potentials are the average of 16 leaves (four leaves per tree, four trees per site). The inverse of the slopes of the linear regressions through the data points were used for calculating G_t and $G_{t,LA}$ for each site (Table 3) according to Eqs. (2) and (4) in the text, respectively. Slopes are significantly different ($P < 0.05$) in (A) only.

applied concurrently to both upland and lowland canopies. Overall, changes in parameters that lead to a decrease in soil–root–leaf pathway hydraulic conductance resulted in an increase in Q. Discharge is most sensitive to the seasonal maximum LAI, Ψ_{min}, and root resistivity. Discharge decreased as the total root length (m) in the soil column increased. Discharge was least responsive to changes in stem conductance, the amount of nitrogen (N) per unit leaf area, and stem capacitance.

5. Discussion

5.1. Observations of plant–water relations across the topographic gradient

The dominant species in the Cascade Brook watershed, *Q. rubra*, displayed significant differences in water relations and morphology at our two sites across the topographic gradient. Drought adapted upland trees exhibited a reduction in stomatal conductance (Fig. 3), sapflow (Fig. 4), height, and leaf to sapwood area ratios (A_L:A_S, Table 3) relative to the trees in lowland areas. The sensitivity to VPD was also reduced in trees at the upland site, agreeing with previous observations on this species (Kubiske and Abrams, 1992). No significant differences in average mid-day Ψ_L values (Table 2) were found between the upland and lowland sites, indicating that the minimum allowable water potential (Ψ_{min}) required for physiological processes is similar for upland and lowland trees. Stand-level hydraulic conductance per unit leaf area ($G_{t,LA}$, Fig. 5) was not significantly different between the upland and lowland sites despite the differences in total leaf area and stem density (Table 3). These results suggest an adaptation of tree morphology and leaf-level gas exchange such that soil–leaf water potential gradients are similar throughout the watershed. These results also suggest a homeostatic relationship (e.g. Margolis et al., 1988) involving stand-level A_L:A_S, stem density, and soil moisture conditions that lead to upland–lowland similarities in the leaf–area specific canopy water use.

Since $G_{t,LA}^{upland} \cong G_{t,LA}^{lowland}$, and since g_s and $G_{t,LA}$ are both measures of tree water use per unit leaf area, it would be expected that $g_s^{upland} \cong g_s^{lowland}$. However, consistent with the observations of Turnbull et al. (2001), g_s in upper-canopy leaves was generally higher at the lowland site. While $G_{t,LA}$ is determined from sapflow measured at the tree base, g_s is measured at the leaf level. Conducting leaf level measurements throughout the

Table 3
Stand structural properties and average individual tree morphological characteristics of *Q. rubra* in the Cascade Brook watershed

Characteristic	Upland site	Lowland site	Units
Stand level			
Basal area[1]	4.8	10.3	m^2 ha^{-1}
Stem density[1]	170	100	stems ha^{-1}
Leaf area index (LAI)[2]	1.55	2.1	m^2 m^{-2}
Leaf: sapwood area (A_L:A_S)[3]	1.2[a]	1.7[b]	10^4 m^2 m^{-2}
Hydraulic conductance*(G_t)	3.3[a]	5.3[b]	10^{-6} kg m^{-2} s^{-1} MPA^{-1}
Relative conductivity (k)	2.85×10^{-13}[a]	8.27×10^{-13}[b]	m^2
Leaf area-specific conductance[3] ($G_{t,LA}$)	0.22[a]	0.25[a]	10^{-5} kg m^{-2} s^{-1} MPA^{-1}
Average individual			
Height (h)[3]	10	20	m
Basal area (A_T)[3]	647 (124)	1123 (146)	cm^2
Total sapwood (A_S)[3]	117 (18)[a]	131 (7)[a]	cm^2
A_S:A_T[3]	0.20 (0.02)[a]	0.10 (0.01)[b]	m^2 m^{-2}
Specific leaf area[1]	11.5 (0.51)[a]	13.0 (0.46)[b]	m^2 kg^{-1}
Mid-day leaf–soil water potential gradient[3]	1.65 (0.1)[a]	1.53 (0.1)[a]	MPA
Maximum stomatal conductance[3] (g_s)	0.33	0.42	mol m^{-2} s^{-1}

Coefficients a and b designate statistically significant differences ($P<0.05$) in values across sites.
* Expressed per unit ground area.
[1] Turnbull et al. (2001).
[2] K. Brown, unpublished data.
[3] This study.

Table 4
Model parameters used to simulate hydrologic fluxes in the Cascade Brook watershed

Parameter	Upland canopy	Lowland canopy
Percent area coverage (%)	75	25
Minimum leaf water potential (Ψ_{min}, MPa)[a]	−2.7	−2.7
Seasonal maximum leaf area index ($m^2\ m^{-2}$)[b]	4	5.5
Rooting depth (m)[d]	0.5	1
Areal foliar N concentration (g N m^{-2})[c]	4.9	6.5
Maximum carboxylation rate (V_{cmax}, μmol CO_2 m^{-2} s^{-1})[c]	54	47
Maximum electron transport rate (J_{max}, μmol CO_2 m^{-2} s^{-1})[c]	133	135
Canopy height (h, m)[a]	10	20
Root resistivity (R_r^*, MPA s m $mmol^{-1}$)[d]	200	200
Canopy layer capacitance (C_n, mmol m^{-2} MPA^{-1})[d]	8000	16 000
Total root length (m m^{-2})[d]	1200	1000

All other parameters necessary to initialize the SPA canopy model as in Williams et al. (1996) and Williams et al. (2001).
[a] Observation.
[b] K. Brown personal communication.
[c] Turnbull et al. (2001).
[d] Estimated.

canopy, and not just at the canopy top, may eliminate this apparent discrepancy. Measurements of g_s at the lowland site revealed a $\sim 50\%$ decrease from upper to mid-canopy leaves. The stand average g_s for *all* leaves at this site is therefore likely to be less than the upper-canopy values reported in Fig. 3. A lower stand average g_s at the lowland site would eliminate the discrepancy between observations of leaf-level measurements and $G_{t,LA}$. We did not make mid-canopy measurements of g_s at the upland site. However, the openness and lack of crown interference from neighboring trees at this site creates a more even light environment in lower canopy layers. This would tend to reduce spatial variability in g_s and suggests the upper-canopy measurements at the upland site are more representative of the local stand average. The morning hours show the largest upland–lowland differences in upper-canopy g_s values and may be due to a greater contribution of xylem storage in the larger lowland trees helping to maintain higher g_s during these periods.

The lowland trees showed an increased sensitivity to VPD relative to the upland trees. Although g_s and sapflow were higher in lowland trees, both declined in response to increasing VPD more quickly than in upland trees (Figs. 3 and 4). Lowland trees exhibited late-afternoon declines in sapflow associated with increasing VPD several hours earlier than upland trees. At the upland site, the near-maximum sapflow sustained during late-afternoon hours coincides with a decreased sensitivity of g_s to increases in VPD. Correlations between maximum g_s and sensitivity to VPD have been reported for many other species (Morison and Gifford, 1983; Yong et al., 1997; Oren et al., 1999).

The morphology of the upland trees suggests a long-term adjustment in carbon allocation in response to lower soil moisture. By decreasing A_L:A_S, stem resistance on a leaf area basis is reduced (Whitehead et al., 1984). The height reduction in upland trees also lowers their hydraulic resistance. These morphological features produce xylem flow sufficient to meet the evaporative demand at the leaf surface with mid-day Ψ_L values similar to those found in lowland trees. Upland trees may also be less prone to cavitation than the lowland trees. The risk of cavitation generally decreases with declining xylem hydraulic conductivity if this decline is also accompanied by a reduction in g_s. Measured hydraulic conductivity (k, Table 3) is lower in the upland trees, which may explain the observations of lower g_s at this site. The apparent trade-off between xylem conducting capacity (represented by k) and the susceptibility to cavitation has been the subject of several recent investigations (Sperry et al., 1998; Nardini and Tyree, 1999; Pinol and Sala, 2000).

The lowered risk of cavitation might also explain the reduced sensitivity to VPD observed in the upland trees (Oren et al., 1999).

When applied to stem segments, k is a measure of xylem-specific conductance (total water use divided by xylem cross-sectional area) and is often equated with the permeability of xylem tissue. Permeability is a function of xylem anatomical characteristics such as vessel length and diameter (Zimmermann, 1983; Tyree and Ewers, 1991). According to Eq. (3), however, in-situ k values are a measure of the complete soil–leaf pathway and implicitly include the soil hydraulic conductivity (k_{soil}; Breda et al., 1993). Soil hydraulic conductivity typically decreases with moisture content, and the reduced soil moisture at the upland site may have biased our estimates of k at this site toward lower values. Without independent measurements, therefore, we cannot attribute upland–lowland differences in k to changes in xylem anatomy or to the lower soil moisture conditions at the upland site. Evidence for the genetic control on xylem conductivity has been reported elsewhere (Zimmermann, 1983; Vander Willigen et al., 2000), though developmental changes in xylem conductivity in response to environmental factors have also been reported (Read and Farquhar, 1991). Assuming no differences in xylem anatomy between the upland and lowland trees, the lower k observed at the upland site would most likely be due to reduced soil moisture. Under well-watered conditions, therefore, the lower A_L:A_S at the upland site suggests these trees are capable of a *higher* leaf area-specific conductance ($G_{t,LA}$) relative to the lowland trees. Observations supporting this conclusion earlier in the growing season indicated canopy water use per unit ground area was approximately equal between sites immediately

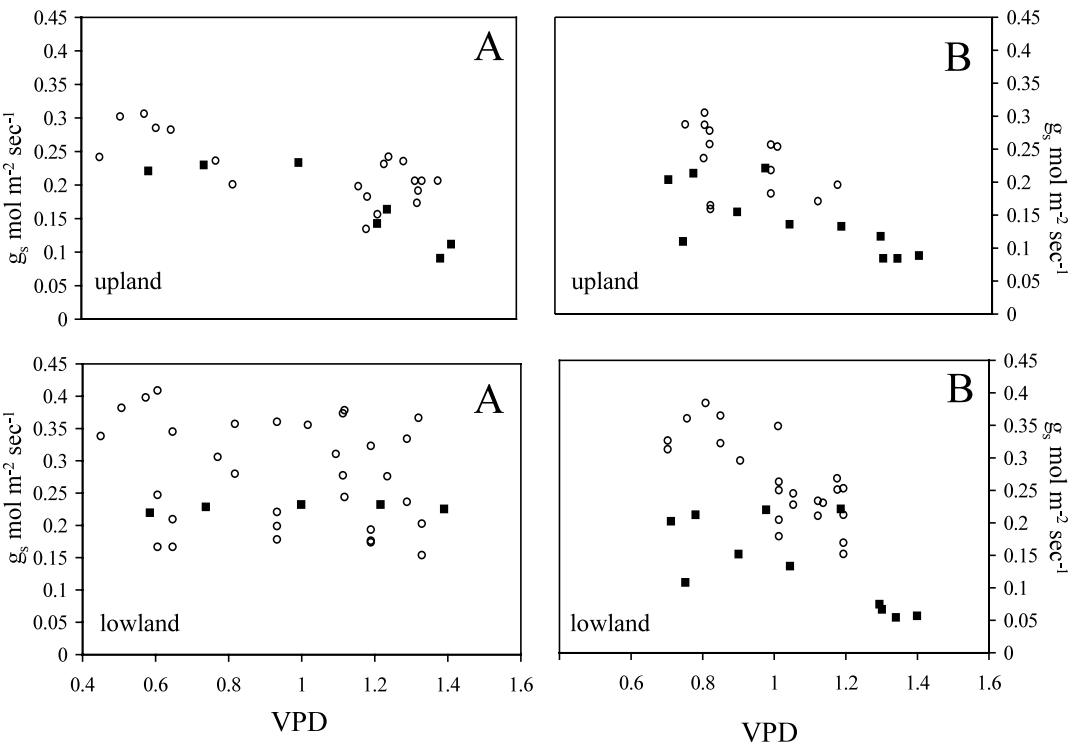

Fig. 6. Comparison of modeled (squares) and observed (circles) stomatal conductance rates as a function of VPD on (A) September 20th and (B) September 21st in upland and lowland canopies. Each observational data point represents the mean value of measurements taken from four leaves on an individual tree. Data from four trees at each site are included in the graphs. Lowland data include observations of g_s measured in mid-canopy leaves.

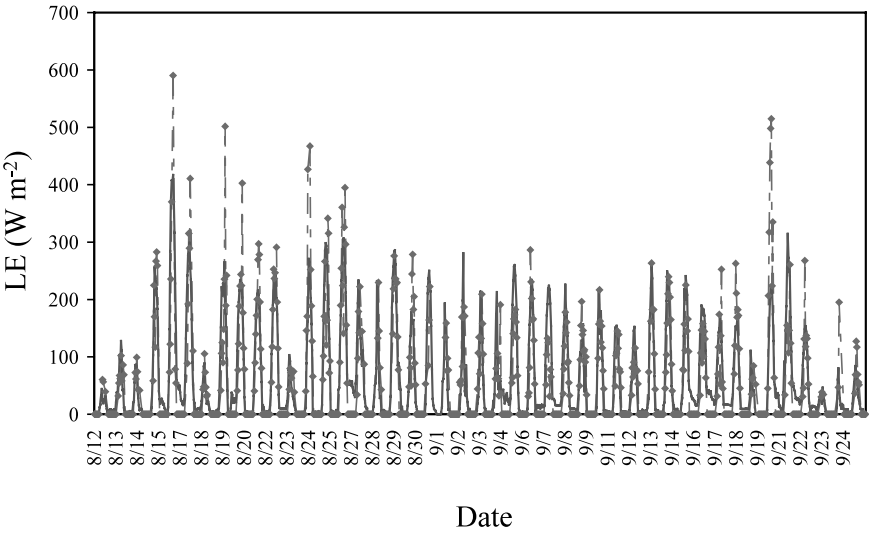

Fig. 7. Comparison of modeled and observed hourly latent energy fluxes (W m^{-2}) during July and August 2000. The observations of LE (dashed line with symbols) were derived from the Bowen ratio measurements at the upland site and compared with model LE (sum of upland canopy transpiration and soil surface fluxes from f_{unsat}). See Section 5 for explanation of discrepancies between observations and model results.

following rain events. Higher g_s rates in *Q. rubra* xeric versus mesic ecotypes have previously been reported under well-watered conditions (Kubiske and Abrams, 1992). The development of stems with high hydraulic efficiency in uplands would enable maximum carbon gain when soil moisture is not limiting and the soil–root resistance is reduced.

While water-use in the upland site appears to be limited by conductivity at the soil–root interface, the data suggests this may not be the case at the lowland site. This site is characterized by increased soil moisture, a deeper soil column, and proximity to the stream draining the system. The lowland trees are significantly taller, and the data suggest that leaf level gas exchange and water-use in these trees is limited instead by xylem conductance. The rapid decline in sapflow observed in the lowland trees during periods of mid-day peak evaporative demand has been attributed to reductions in xylem conductivity for several other species (Ryan and Yoder, 1997; Schafer et al., 2000). The increased response of g_s to VPD at this site also supports this hypothesis. While xylem storage may contribute to the higher g_s during morning hours at the lowland site, stomata must close during periods of high evaporative demand in order to maintain Ψ_L above Ψ_{min}.

In summary, the observational data indicate a complex interaction of stand structure, tree morphology, g_s, and soil moisture. The upland trees are shorter, have a lower A_L:A_S, and show reduced sensitivity to VPD compared to lowland trees. The morphology and lower transpiration rates of the upland trees maintain soil–leaf water potential gradients close to those observed at the lowland site despite the reduced soil moisture conditions. Although the rate of sapflow in individual trees is diminished at the upland site, there are more trees per unit ground area and a lower LAI in this area. This stand structure produces a canopy-level $G_{t,LA}$ during mid-day conditions very similar to that found at the lowland site (Fig. 5B). This observation suggests a stand-level adjustment that governs the rate of water use on a leaf-area basis similarly in the upland and lowland communities. Further observations are necessary to determine the degree of drought stress that might cause deviations from this pattern. Drier conditions are likely to induce stomatal closure at the upland site and reduce $G_{t,LA}$ below lowland values.

The growth patterns and morphology of the lowland trees, less restricted by soil moisture availability than in the upland trees, appears instead to be dominated by competition for light. This competition leads to an average canopy height approximately two times taller than in upland areas. The increased path length resistance associated with the height of the lowland trees, however, may limit the ability of the xylem to meet high evaporative demand at the leaf surface. An increased stomatal sensitivity to VPD at the leaf surface is therefore necessary to control transpirational losses and to maintain favorable leaf water status.

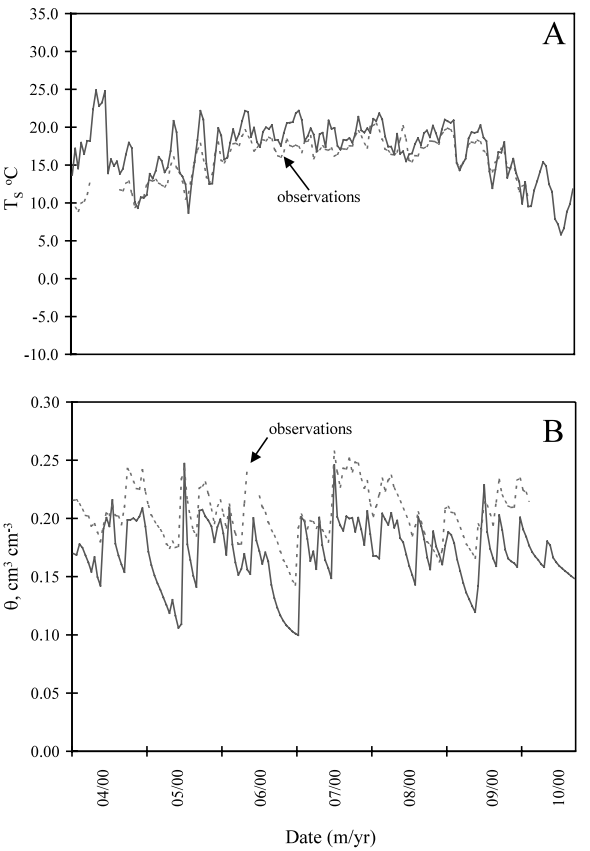

Fig. 8. Comparisons of modeled and observed soil temperature and moisture contents. Simulated (solid lines) and observed average daily values for (A) soil temperatures, and (B) soil moisture, θ, from April to October 2000. Observations were compared to the average values of the top five model layers ($\sim$20 cm) for θ and to the top three model layers ($\sim$10 cm) for T_S. These depths correspond to the positions of the soil moisture and temperature sensors.

Taken together, these results show how transpiration rates and the utilization of soil moisture in this watershed are linked to both the minimum allowable leaf water potential, Ψ_{min}, in *Q. rubra* and to the morphological adaptations in the upland and lowland trees necessary to meet this requirement. Individual tree morphology and overall stand structure thus reflect the topographic control over soil moisture distribution in this catchment. Leaf-level gas exchange rates, land surface–atmosphere interactions, and runoff are similarly affected by topographic controls. These observations directed the development of the model and justified the inclusion of separate upland and lowland canopies in simulations. In this way, the topographic control over soil moisture, the dynamics of the soil–root–leaf pathway and runoff could be simulated in a consistent framework.

5.2. Model performance

We validated the model with stomatal conductance, g_s (Fig. 6), upland latent heat flux, LE (Fig. 7), whole-watershed averaged surface soil temperatures, T_S, and soil moisture, θ (Fig. 8), and discharge, Q (Fig. 9). The model predictions of Q in this watershed were very similar to the predictions of Q from Shaman et al. (2001) using the model of Stieglitz et al. (1997). Predictions of soil moisture conditions and discharge compared favorably with observations and provided confidence the model was capturing the dynamics of the local hydrologic cycle over daily time scales. Latent heat flux comparisons at hourly scales were also encouraging, but subject to greater discrepancies. A significant portion of the discrepancy between model results and observations may have resulted from uncertainty in the Bowen ratio measurements. Errors were most likely due to advection of sensible and latent heat from other areas, and the difficulty in resolving vapor pressure gradients above aerodynamically rough surfaces. Despite these difficulties there was some agreement between modeled and observed values during periods of low LE flux. Agreements gener-

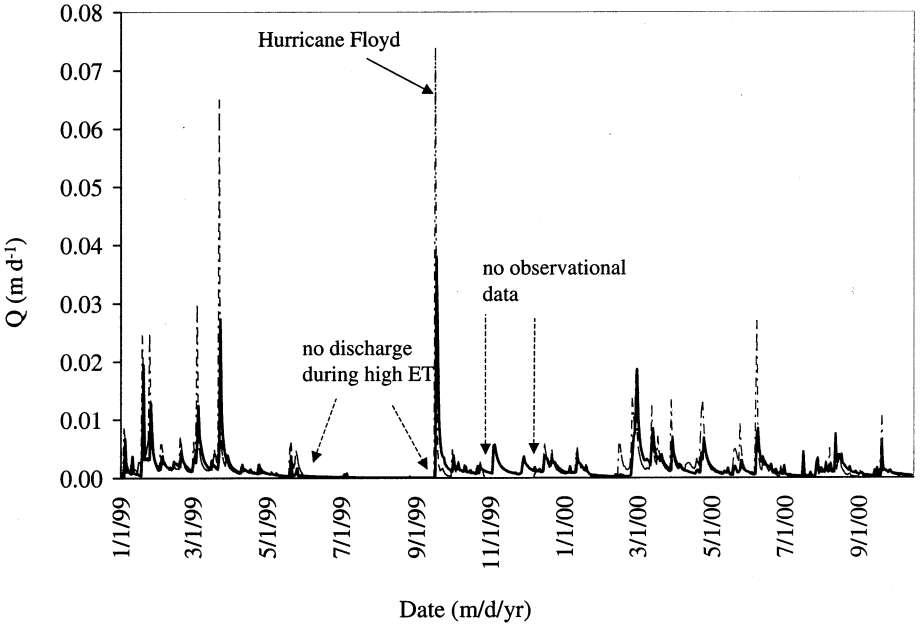

Fig. 9. Simulated (solid line) and observed daily discharge rates (Q) from the Cascade Brook watershed from January 1999 to October 2000. From June to September 1999, discharge over the weir stopped in response to high evaporative demand and low rainfall. Flow in Cascade Brook did not resume until Hurricane Floyd arrived on September 16th, 1999. During Floyd a significant percentage of runoff overflowed the weir through a temporary drainage channel, making comparisons with model results inconclusive during this event.

ally occurred during morning and evening hours under more stable atmospheric conditions, when errors associated with advection from other areas would tend to be reduced.

Model predictions of transpiration were sensitive to the value of the stomatal threshold parameter, l (see the model description and Fig. 2) described by Williams et al. (1996). Lower values of this parameter correspond to increased stomatal aperture and reduced water use efficiency. We found an l value of 0.01% produced the best agreement with our site data. Values above 0.01% resulted in lower g_s and an underestimate of LE. In terms of the model dynamics, lowering l had the effect of forcing stomata to open further in response to feedback from smaller incremental gains in photosynthesis (P_n). Likewise, lowering the value of l results in an increase in the maximum g_s, the canopy transpiration, and net photosynthesis.

We used the model to examine differences in upland and lowland transpiration rates (Fig. 10). For these comparisons, the upland canopy fluxes from the unsaturated fraction of the watershed were compared to the lowland canopy fluxes from the saturated fraction. In this way, the interactive effects of soil moisture and canopy morphology (different for the upland and lowland canopies) on transpiration rates could be analyzed. During periods of low root zone (the top 0.5 m of the 1-D soil column) soil moisture conditions in the uplands, high soil hydraulic resistance restricted transpiration relative to the lowland areas. During periods of very high VPD, however, transpiration in the saturated, lowland canopy was reduced relative to the upland canopy. This response occurred due to the differences in morphology prescribed for the two canopies. The height of the lowland trees was set at two times the value for the upland trees and with a higher LAI. As a result of the higher leaf area, the total evaporative demand (VPD times the total leaf area) for the lowland canopy is greater than for the upland canopy. Despite the saturating soil moisture con-

ditions, increased capacitance, and higher xylem conductance for the lowland canopy, evaporative demand exceeded the supply from the soil–root–xylem pathway, thereby forcing stomata to close. That is, the increased height of the lowland canopy results in an increase in xylem resistance and a hydraulic limitation on g_s during periods of high VPD. Our observations, in general, support this model result. Our observations also support the model results showing upland–lowland similarities in hydraulic conductance per unit leaf area ($G_{t,LA}$, Table 3 and Fig. 11). The SPA canopy model is not designed explicitly to generate this result. Instead, the upland–lowland similarities in $G_{t,LA}$ and soil–leaf water potential gradients ($\Psi_S - \Psi_L - h\rho g$) generated by the coupled model are a property of the calculated transpiration rates, the canopy morphologies and the soil moisture content in the f_{sat} and f_{unsat} area fractions. While our period of observations was somewhat

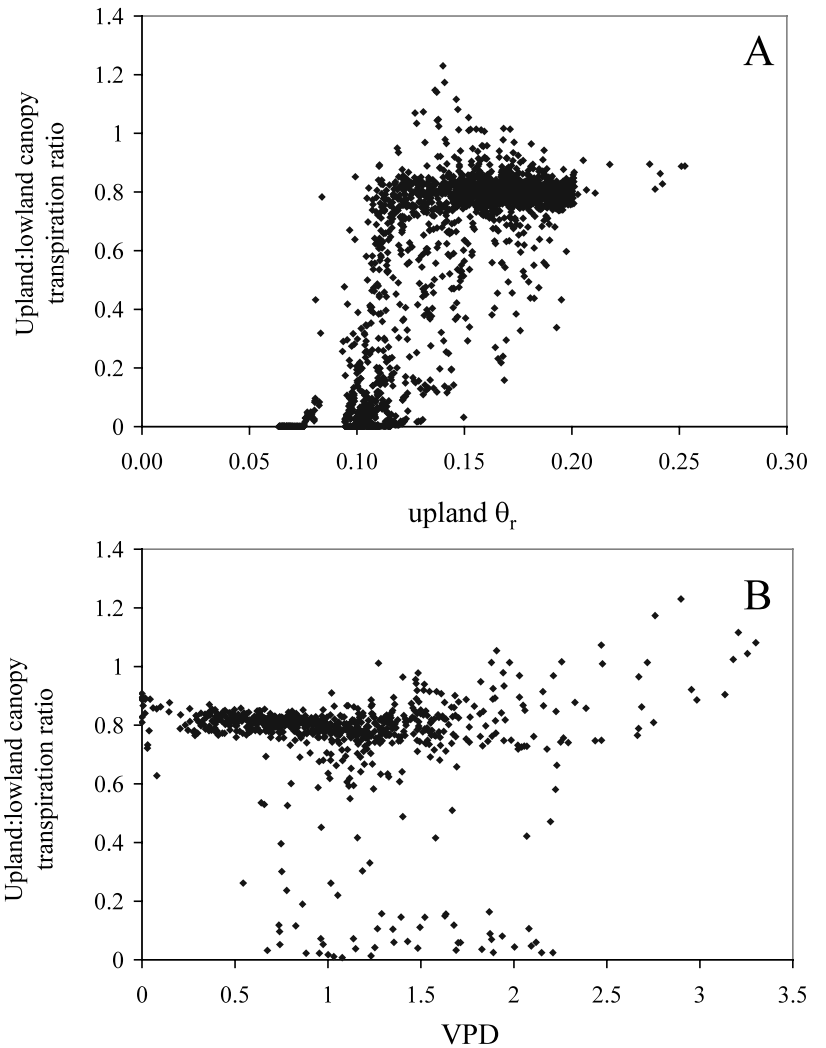

Fig. 10. Ratios of modeled upland and lowland canopy transpiration rates. Ratios are plotted as a function of (A) upland canopy root-zone soil moisture θ_r and (B) atmospheric vapor pressure deficit. Low ratios occur during drought periods when θ_r is reduced below 0.15 $cm^3\ cm^{-3}$. Under most soil moisture conditions, upland transpiration rates are approximately 0.8 times lowland rates. Upland:lowland transpiration ratios above 1 occur only during the highest VPD conditions.

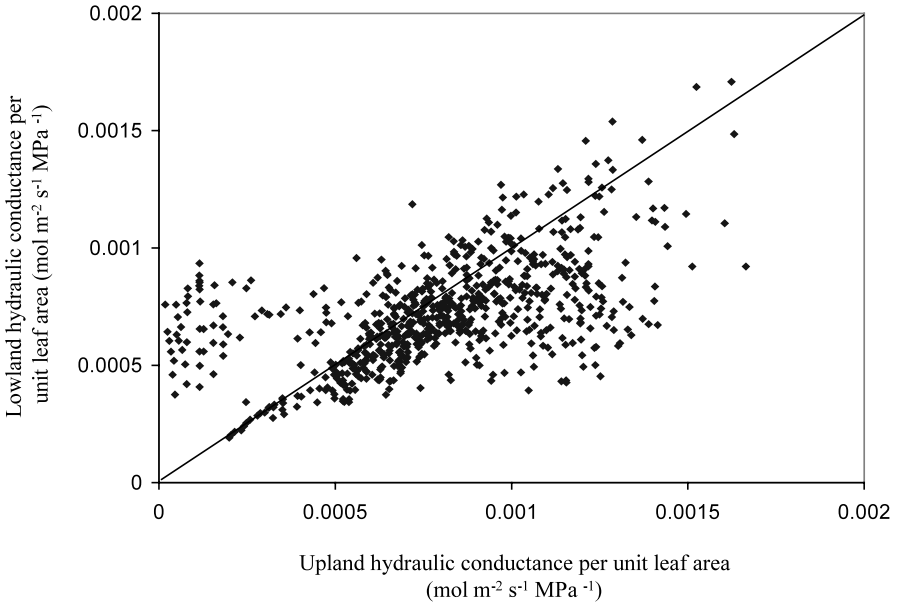

Fig. 11. Comparison of hourly values of upland and lowland hydraulic conductance per unit leaf area, $G_{t,LA}$, for the 2000 growing season. Points were calculated as in Eq. (4) in the text, using modeled rates of total transpiration, the weighted leaf-water potential (average for all canopy layers based on leaf area distribution and layer water potential), and the leaf area index for each site. The 1:1 line is included for reference purposes.

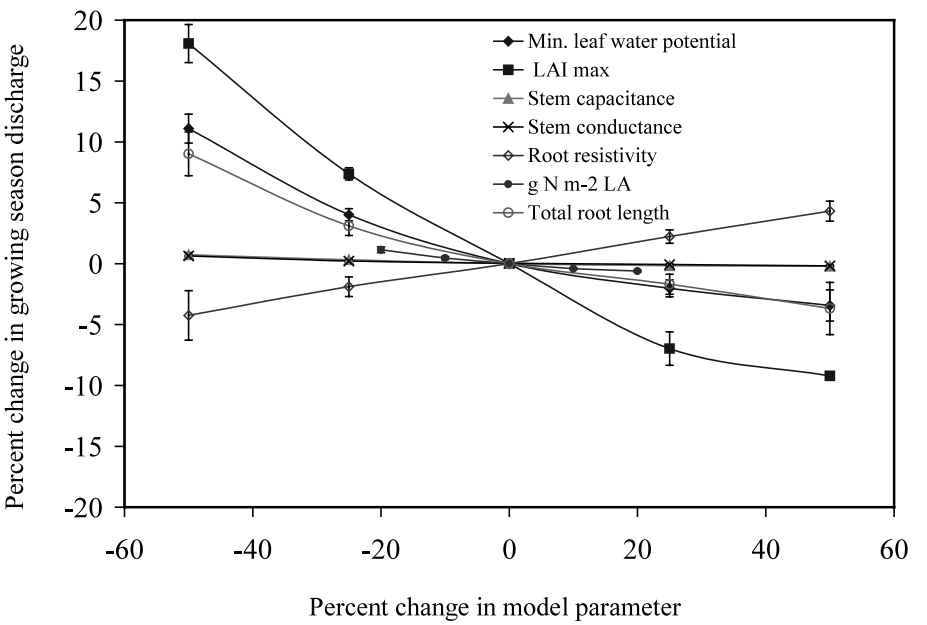

Fig. 12. Sensitivity of stream discharge to changes in canopy hydraulic parameters. Average percent differences from baseline values (see Table 4) are shown on the horizontal axis. The percent changes in model parameters were applied equally across the upland- and lowland-type canopies. Parameters were varied individually. Results are averaged over the 1998, 1999, and 2000 growing seasons.

limited, the data indicated a close similarity in upland–lowland $G_{t,LA}$. The model results suggest the upland–lowland similarities in $G_{t,LA}$ values, while close to the observed 1:1 ratio for many periods, do deviate during low soil moisture (θ_r) conditions ($G_{t,LA}^{upland} < G_{t,LA}^{lowland}$). During periods of moderate soil moisture stress, $G_{t,LA}^{upland}$ is often greater than $G_{t,LA}^{lowland}$.

We employed a sensitivity analysis to identify those components of the soil–root–leaf pathway that impact stream discharge (Fig. 12). Discharge was chosen because it reflects the integrated response to the ecosystem water status. Discharge is routinely recorded and readily available for many streams—making it a useful diagnostic tool for the performance of the model. The results indicate modeled discharge is most sensitive to canopy parameters that increase the hydraulic transport capacity (e.g. increasing soil or root conductivities), and to those that lead to changes in evaporative demand at the leaf surface (e.g. increasing seasonal maximum LAI or lowering Ψ_{min}). In general, stream discharge rates displayed greater sensitivity to model parameters that reduced, rather than increased, the canopy hydraulic conductance. This was most obvious for seasonal LAI, where a 50% decrease in the seasonal maximum LAI resulted in a $\sim$18% increase in discharge, while a 50% increase in LAI caused discharge to decrease by only $\sim$8%. Additional increases in LAI have a proportionally smaller impact on runoff. This is consistent with the coordination of liquid and vapor phase transport in the SPA canopy model. Additional increases in LAI will be accompanied by decreasing g_s in order that minimum leaf water potential is preserved; i.e. to ensure cavitation does not occur. This offsetting impact of decreasing g_s as LAI increases limits total transpiration withdrawals from the soil column, and therefore, the effect on runoff is reduced. These results suggest stomatal limitations on net production are likely to be significant in this system and suggest a close hydrologic control on the long-term carbon balance of this forest.

As with LAI, runoff showed a diminished sensitivity to changes in other model parameters that increased the hydraulic conductance of the soil–root–leaf pathway. The exception was the response of runoff to root resistivity, which was linear over the range of values tested. The lack of change in runoff as canopy hydraulic conductance is increased reflects the water stress conditions that frequently occur during the growing season in this watershed. Dry soil conditions (in both the model and the Cascade Brook watershed) are common during the growing season, and further increases in the ability of the canopy to transpire are not supported due to the lack of available water.

6. Conclusions

Observations showed significant upland–lowland differences in stomatal conductance, sensitivity to VPD, and patterns of sap flux density in sample trees. The observational data also suggest a shift in the primary resistance in the soil–root–leaf pathway from the soil–root interface in upland areas to xylem hydraulic conductance in the lowland areas. This shift in resistance can be used to explain the differences in diurnal patterns of water use observed in the upland and lowland trees. Interestingly, stand-level observations revealed upland–lowland similarities in leaf area-specific canopy hydraulic conductance, suggesting the presence of feedback mechanisms involving individual tree morphology (e.g. height, A_L:A_S), stem density, and soil moisture conditions that govern canopy water use consistently across the local topographic gradient. The coupled model developed for this work presents a methodology for linking the topographic control of soil moisture distribution, atmospheric fluxes and runoff with the hydraulic conductance of the soil–leaf–root pathway. This allows for a computationally efficient approach of examining the hydraulic properties of the soil–leaf–root pathway in the context of whole-watershed hydrology, i.e. the topographic control over surface hydrologic and biologic processes.

Acknowledgements

The authors wish to express their gratitude to Dr. William Schuster and the Black Rock Forest staff for field support and for providing data for

the model simulations. Dr. Kim Brown provided data on leaf area and soil properties. Dr. David Whitehead provided many helpful comments and insights on the data analysis. Dr. David Tissue supplied equipment for the fieldwork. This work was supported by a grant from the Andrew W. Mellon Foundation to KLG, and by two awards from the Columbia University Climate Center (V.C.E., K.L.G. and M.S.). VCE is supported by a fellowship from Columbia University Biosphere 2 Center. This research was also supported by an NSF grant from the division of Environmental Biology (Arctic LTER Project).

References

Ambroise, B., Beven, K., Freer, J., 1996. Toward a generalization of the TOPMODEL concepts: Topographic indices of hydrologic similarity. Water Resour. Res. 32 (7), 2135–2145.

Anderson, E.A., Baker, D.R., 1965. Estimating incident terrestrial radiation under all atmospheric conditions. Water Resour. Res. 3 (4), 975–988.

Band, L.E., Patterson, R., Nemani, R., Running, S.W., 1993. Forest ecosystem processes at the watershed scale: Incorporating hillslope hydrology. Agric. For. Meteor. 63, 93–126.

Beven, K., Kirby, M.J., 1979. A physically based, variable contributing area model of basin hydrology. Hydrol. Sci. J. 24, 43–69.

Beven, K., 1986. Hillslope runoff processes and flood frequency characteristics. In: Abrahams, A.D. (Ed.), Hillslope Processes. Allen and Unwin, pp. 187–202.

Beven, K., 1997. TOPMODEL: A critique. Hydrol. Process. 11 (9), 1069–1085.

Breda, N., Cochard, H., Dreyer, E., Granier, A., 1993. Field comparison of transpiration, stomatal conductance and vulnerability to cavitation of *Quercus petraea* and *Quercus robur* under water stress. Ann. Sci. For. 50, 571–582.

Clearwater, M.J., Meinzer, F.C., Andrade, J.L., Goldstein, G., Holbrook, N.M., 1999. Potential errors in measurement of non-uniform sap flow using heat dissipation probes. Tree Physiol. 19, 681–687.

Ducharne, A.R.D., Koster, R., Suarez, M.J., Stieglitz, M., Kumar, P., 2000. A catchment-based approach to modeling land surface processes in a GCM, Part 2, parameter estimation and model demonstration. J. Geophys. Res. 105, 24823–24838.

Friday, J., Friday, K., 1985. Black Rock Forest Inventory. Harvard Black Rock Forest internal report, 125 pp.

Granier, A., 1985. Une nouvelle methode pour la mesure du flux de seve brute dans le tronc des arbres. Ann. Sci. For. 42, 193–200.

Granier, A., 1987. Evaluation of transpiration in a Douglas-fir stand by means of sap flow measurements. Tree Physiol. 3 (4), 309–320.

Granier, A., Bobay, V., Gash, J.H.C., Gelpe, J., Saugier, B., Shuttleworth, W.J., 1990. Vapour flux density and transpiration rate comparisons in a stand of Maritime pine (*Pinus pinaster* Ait.) in Les Landes forest. Agric. For. Meteorol. 51, 309–319.

Heilman, J.L., Brittin, C.L., Neale, C.M.U., 1989. Fetch requirements for Bowen ratio measurements of latent and sensible heat fluxes. Agric. For. Meteorol. 44, 261–273.

Herbst, M., 1995. Stomatal behaviour in a beech canopy: an analysis of Bowen ratio measurements compared with porometer data. Plant Cell Environ. 18, 1010–1018.

Irvine, M.R., Gardiner, B.A., Hill, M.K., 1997. The evolution of turbulence across a forest edge. Boundary-Layer Meteor. 84 (3), 467–496.

Jarvis, P.G., 1976. The interpretation of the variations in leaf water potential and stomatal conductance found in canopies in the field. Philos. Trans. R. Soc. London 273, 593–610.

Jones, H.G., 1992. Plants and Microclimate. Cambridge University Press, Cambridge, 428 pp

Knight, D.H., Fahey, T.J., Running, S.W., 1985. Water and nutrient outflow from contrasting Lodgepole pine forests in Wyoming. Ecol. Mono. 55 (1), 29–48.

Kubiske, M.E., Abrams, M.D., 1992. Photosynthesis, water relations, and leaf morphology of xeric versus mesic *Quercus rubra* ecotypes in central Pennsylvania in relation to moisture stress. Can. J. For. Res. 22, 1402–1407.

Law, B.E., Williams, M., Anthoni, P., Baldocchi, D.D., Unsworth, M.H., 2000. Measuring and modeling seasonal variation of carbon dioxide and water vapor exchange of a *Pinus ponderosa* forest subject to soil water deficit. Global Change Biol. 6, 613–630.

Liang, W., Lettenmaier, D.P., Wood, E.F., Burges, S.J., 1994. A simple hydrologically based model of land–surface water and energy fluxes for general circulation models. J. Geo. Phys. Res. 99 (D7), 14415–14428.

Margolis, H., Gagnon, R., Pothier, D., Pineau, M., 1988. The adjustment of growth, sapwood area, heartwood area, and sapwood saturated permeability of balsam fir after different intensities of pruning. Can. J. For. Res. 18, 723–727.

Morison, J.I.L., Gifford, R., 1983. Stomatal sensitivity to carbon dioxide and humidity. Plant Physiol. 71, 789–796.

Nardini, A., Tyree, M.T., 1999. Root and shoot hydraulic conductance of seven *Quercus* species. Ann. For. Sci. 56, 371–377.

Newman, E.I., 1969. Resistance to water flow in soil and plant I. Soil resistance in relation to amounts of root: theoretical estimates. J. Appl. Ecol. 6, 1–12.

Oke, T.R., 1987. Boundary Layer Climates. Methuen and Co., New York, NY, 435 pp.

Oren, R., Sperry, J.S., Katul, G.G., Pataki, D.E., Ewers, B.E., Phillips, N., Schafer, K.V.R., 1999. Survey and synthesis of intra- and interspecific variation in stomatal sensitivity to vapor pressure deficit. Plant Cell Environ. 22, 1515–1526.

Parton, W.J., 1993. Observations and modeling of biomass and soil organic matter dynamics for the grassland biome worldwide. Global Biogeochem. Cycles 7, 785–809.

Phillips, N., Oren, R., Zimmermann, R., 1996. Radial patterns of xylem sap flow in non-, diffuse-, and ring-porous tree species. Plant Cell Environ. 19, 983–990.

Pinol, J., Sala, A., 2000. Ecological implications of xylem cavitation for several Pinaceae in the Pacific Northern USA. Funct. Ecol. 14, 538–545.

Pitman, A.J., Yang, Z.-L., Cosley, J.G., Henderson-Sellers, A., 1991. Description of bare essentials of surface transfer for the bureau of meteorological research AGCM, BMRC, Australia. BMRC Research rep. 32.

Read, J., Farquhar, G., 1991. Comparative studies in *Nothofagus* (Fagaceae) l. leaf carbon isotope discrimination. Funct. Ecol. 5, 684–695.

Reich, P.B., Hinckley, T.M., 1989. Influence of pre-dawn water potential and soil-to-leaf hydraulic conductance on maximum daily leaf diffusive conductance in two oak species. Funct. Ecol. 3, 719–726.

Rieger, M., Litvin, P., 1999. Root system hydraulic conductivity in species with contrasting root anatomy. J. Exp. Bot. 50 (331), 201–209.

Running, S.W., Coughlan, J.C., 1988. A general model of forest ecosystem processes for regional applications, I. Hydrologic balance, canopy gas exchange, and primary production processes. Ecol. Model. 42, 125–144.

Ryan, M.G., Yoder, B.J., 1997. Hydraulic limitations to tree height and growth. Bioscience 70 (4), 235–242.

Saliendra, N.Z., Sperry, J.S., Comstock, J.P., 1995. Influence of leaf water status on stomatal response to humidity, hydraulic conductance, and soil drought in *Betula occidentalis*. Planta 196, 357–366.

Schafer, K.V.R., Oren, R., Tenhunen, J.D., 2000. The effect of tree height on crown level stomatal conductance. Plant Cell Environ. 23, 365–375.

Sellers, P.J., Randall, D.A., Collatz, G.J., Berry, J.A., Field, C.B., Dazlich, D.A., Zhang, C., Collelo, G.D., Bounoua, L., 1996. A revised land surface parameterization (SiB2) for atmospheric GCMs. Part I: Model Formulation. Journal of Climate 9 (4), 676–705.

Shaman, J., Stieglitz, M., Engel, V.C., Koster, R., Stark, C., 2001. Representation of stormflow and a more responsive water table in a TOPMODEL-based hydrology model. Water Resour. Res., submitted for publication.

Sivapalan, M., Beven, K., Wood, E.F., 1987. On hydrologic similarity 2, a scaled model of storm runoff production. Water Resour. Res. 23 (12), 2266–2278.

Stieglitz, M., Rind, D., Famiglietti, J., Rosenzweig, C., 1997. An efficient approach to modeling the topographic control of surface hydrology for regional and global climate modeling. J. Climate 10, 118–137.

Sperry, J.S., Adler, F.R., Campbell, G.S., Comstock, J.P., 1998. Limitation of plant water use by rhizosphere and xylem conductance: results from a model. Plant Cell Environ. 21, 347–359.

Turnbull, M.H., Whitehead, D., Tissue, D.T., Schuster, W., Brown, K.J., Engel, V.C., Griffin, K.G., 2002. Photosynthetic characteristics in canopies of Quercus rubra, Quercus prinus, and Acer rubrum differ in response to soil water availability. Oecologia 130, 515–524.

Tyree, M.T., Sperry, J.S., 1988. Do woody plants operate near the point of catastrophic xylem dysfunction caused by dynamic water stress? Plant Physiol. 88, 574–580.

Tyree, M.T., Ewers, F.K., 1991. The hydraulic architecture of trees and other woody plants. New Phytol. 119, 345–360.

Vander Willigen, C., Sherwin, H.W., Pammenter, N.W., 2000. Xylem hydraulic characteristics of subtropical trees from contrasting habitats grown under identical environmental conditions. New Phytol. 145, 51–59.

Whitehead, D., Jarvis, P.G., Waring, R.H., 1984. Stomatal conductance, transpiration, and resistance to water uptake in a *Pinus sylvestris* spacing experiment. Can. J. For. Res. 14, 692–700.

Whitehead, D., 1998. Regulation of stomatal conductance and transpiration in forest canopies. Tree Physiol. 18, 633–644.

Whitehead, D., Leathwick, J.R., Walcroft, A.S., 2001. Modeling annual carbon uptake for the indigenous forests of New Zealand. For. Sci. 42, 1.

Wigmosta, M.S., Vail, L.W., Lettenmaier, D.P., 1994. A distributed hydrology–vegetation model for complex terrain. Water. Resour. Res. 30 (6), 1665–1679.

Williams, M., Rastetter, E.B., Fernandes, D.N., Goulden, M.L., Wofsy, S.C., Schaver, G.R., Melillo, J.M., Munger, J.W., Fan, S.-M., Nadelhoffer, K.J., 1996. Modelling the soil–plant–atmosphere continuum in a *Quercus–Acer* stand at Harvard Forest: the regulation of stomatal conductance by light, nitrogen, and soil/plant hydraulic properties. Plant Cell Environ. 19, 911–927.

Williams, M., Law, B.E., Anthoni, P.M., Unsworth, M.H., 2001. Use of a simulation model and ecosystem flux data to examine carbon–water interactions in ponderosa pine. Tree Physiol. 21, 287–298.

Wood, E.F., Sivapalan, M., Beven, K., 1990. Similarity and scale in catchment storm response. Rev. Geophys. 28 (1), 1–18.

Wullschleger, S.D., Meinzer, F.C., Vertessy, R.A., 1998. A review of whole-plant water use studies in trees. Tree Physiol. 18, 499–512.

Yong, J.W.H., Wong, S.C., Farquhar, G., 1997. Stomatal response to changes in vapor pressure difference between leaf and air. Plant Cell Environ. 20, 1213–1216.

Zimmermann, M.H., 1983. Xylem Structure and the Ascent of Sap. Springer-Verlag, Berlin.